Anthropocene 53 (2026) 100504

Contents lists available at ScienceDirect

Anthropocene

journal homepage: www.elsevier.com/locate/ancene

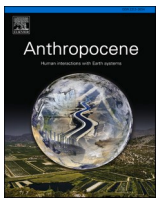

Five centuries of lake deoxygenation and microbial shifts revealed by sedimentary DNA

Teresa Vegas-Vilarrúbia [a,*], Oriol Sacristán-Soriano [b,i], Carles M. Borrego [b,c], Juan Pablo Corella [d], Paz Errea [e], Teresa Buchaca [f], Valentí Rull [g,h]

[a] Department of Evolutionary Biology, Ecology and Environmental Sciences, Universitat de Barcelona, Av. Diagonal 643, Barcelona 08028, Spain
[b] Institut Català de Recerca de l'Aigua (ICRA), Emili Grahit 101, Girona E-17003, Spain
[c] Grup d'Ecologia Microbiana Molecular, Institut d'Ecologia Aquàtica, Universitat de Girona, Campus de Montilivi, Girona E-17003, Spain
[d] National Museum of Natural Sciences-CSIC, Serrano 115 bis, Madrid 28006, Spain
[e] Instituto Pirenaico de Ecología, IPE, Zaragoza, Spain
[f] Integrative Freshwater Ecology, Centre for Advanced Studies of Blanes (CEAB-CSIC), Spain
[g] Institut Botànic de Barcelona, Spanish National Research Council (CSIC), Pg.del Midgia s/n, Barcelona 08038, Spain
[h] Institut Català de Paleontologia Miquel Crusafont, Universitat Autònoma de Barcelona, C. de les Columnes s/n, ICTA-ICP Bld., Cerdanyola del Vallès, 08193, Spain
[i] Technological Centre in Biodiversity, Ecology and Environmental and Food Technology, University of Vic–Central University of Catalonia (CT BETA UVic-UCC), Spain

ARTICLE INFO

Keywords:
Anthropocene
Climate change
Community responses
Hypoxia
Hemp retting
Functional resilience

ABSTRACT

Expanding global deoxygenation is a major ecological crisis. Oxygen loss in aquatic systems is reshaping ecosystems, altering biodiversity, nutrient cycles, and ecosystem functioning. Microbial communities, as key biogeochemical mediators, are highly responsive to oxygen availability, yet their long-term trajectories under sustained oxygen loss remain poorly understood. This limits our ability to anticipate ecosystem responses to climate-driven deoxygenation. We reconstructed five centuries of microbial and oxygen dynamics in meromictic Lake Montcortès (southern Pyrenees) using sedimentary deoxyribonucleic acid (DNA) and X-ray fluorescence spectroscopy of varved sediments. Average volume of anoxic water (VAW) increased from 545,560 m^3 in the preindustrial period (1500–1750 Common Era) to 558,692 m^3 after 1905, with greater persistence from 1937 onward. Instrumental data (2013–2020) confirmed this trend, with VAW peaking at 1018,400 m^3 and anoxia reaching 11.5 m and anoxia occurring below 11.5 m depth. Microbial communities gradually shifted from suboxic-adapted taxa to anaerobic assemblages dominated by sulfate-reducing bacteria and methanogenic archaea, reflecting historical anthropogenic pressures and recent warming-driven anoxia. Despite compositional change, core functional traits persisted, with no evidence of abrupt regime shifts indicating microbial resilience under long-term redox stratification. The timing of stratification intensification in Lake Montcortès coincides with the mid-20th century onset of the Anthropocene, as defined by the Anthropocene Working Group. Its annually resolved varved sediments, combined with clear geochemical and microbial signals of anthropogenic impact, support its proposal as a candidate Global Boundary Stratotype Section and Point Global (GSSP or "golden spike").

1. Introduction

Deoxygenation is a growing global concern in both marine and freshwater systems, with profound implications for biodiversity, biogeochemical cycling, and ecosystem functioning. Driven by eutrophication, climate warming, and altered stratification patterns, oxygen loss is increasing in frequency, duration, and spatial extent (Breitburg et al., 2018; Jane et al., 2021). Given its critical role in regulating Earth system stability, deoxygenation has recently been proposed as a new planetary boundary (Rose et al., 2024).

In freshwater ecosystems, climate-induced changes in thermal regimes enhance water column stability and reduce vertical mixing, limiting oxygen replenishment and increasing the risk of long-term or permanent hypoxia (Ficker et al., 2017; Jane et al., 2021, 2023; Tu et al.,

* Corresponding author.
E-mail addresses: tvegas@ub.edu (T. Vegas-Vilarrúbia), oriol.sacristan@uvic.cat (O. Sacristán-Soriano), cborrego@icra.cat, carles.borrego@udg.edu (C.M. Borrego), pablo.corella@mncn.csic.es (J.P. Corella), paz@ipe.csic.es (P. Errea), buch@ceab.csic.es (T. Buchaca), vrull@csic.es, Valenti.rull@icp.ca (V. Rull).

https://doi.org/10.1016/j.ancene.2025.100504
Received 2 August 2025; Received in revised form 13 November 2025; Accepted 28 November 2025
Available online 29 November 2025

2024; Zhang et al., 2025). These conditions alter nutrient dynamics and impair redox-sensitive processes such as carbon burial and sulfur and iron cycling. While the short-term impacts of oxygen depletion are relatively well documented, its long-term ecological consequences—particularly in relation to microbial community dynamics—remain insufficiently understood.

Deoxygenation in aquatic systems arises from complex biogeochemical and hydrological interactions that operate across multiple timescales Although seasonal (Bush et al., 2017) and interannual (Ladwig et al., 2021) oxygen fluctuations have been widely studied, long-term variability over decadal to centennial timescales remains poorly characterized (Jenny et al., 2016; Vegas-Vilarrúbia et al., 2018). These extended timescales are critical, as they align with major climate shifts and cumulative anthropogenic influences that can drive sustained oxygen loss. Although anoxia may develop within a single stratification season in eutrophic lakes, its persistent expansion typically unfolds over decades to centuries. Reconstructing past oxic-anoxic transitions is essential to understanding contemporary oxygenation patterns and anticipating future trajectories.

The progressive expansion of anoxic waters raises serious ecological concerns, including mass die-offs of eukaryotic organisms and the buildup of toxic anaerobic by-products such as sulfide and methane. Over extended periods, such conditions promote the establishment of anaerobic microbial assemblages and the formation of persistent "dead zones" (Bush et al., 2017). Investigating how microbial communities respond to long-term oxygen fluctuations offers critical insight into the ecological transformations associated with sustained deoxygenation

The meromictic nature of Lake Montcortès (Central Pyrenees, Spain) provides a natural model for studying long-term oxic-anoxic shifts. The monimolimnion has remained anoxic for extended periods (Vegas-Vilarrúbia et al., 2018, 2020), supporting stable anaerobic habitats for microbial communities. Stratigraphic analyses confirm persistent deep-water anoxia, and the lake's varved sediments offer high-resolution records of ecological, environmental, and climatic change (Corella et al., 2014, 2019; Rull et al., 2023; Vegas-Vilarrúbia et al., 2022). Their fine structure, low porosity, and lack of bioturbation promote in-situ preservation of microbial DNA, enabling reconstruction of past communities. Given the annual-resolution dating of the last century and prior studies, Lake Montcortès has been proposed as a sequence potentially containing the lower Anthropocene boundary, as defined by the Anthropocene Working Group (AWG), coinciding with the Great Acceleration (mid-20th century) (Rull et al., 2023).

We hypothesize that variations in lake stratification, climate fluctuations, and anthropogenic disturbances shaped the anaerobic conditions of the hypolimnion in Lake Montcortès from 1500 to 2011. These factors may have acted independently or synergistically over time, driving distinct shifts in microbial community composition. We further propose that examining long-term anoxic conditions and microbial dynamics in this lake offers valuable insights into the ecological consequences of ongoing freshwater deoxygenation—both present and future. To test these hypotheses, we aimed to: i) reconstruct historical changes in hypolimnetic oxygenation using geochemical indicators; ii) infer shifts in bacterial community assemblages through sedimentary DNA analysis; iii) evaluate the impact of multiple environmental disturbances on microbial dynamics; and iv) integrate palaeoecological, palaeoenvironmental, and palaeoclimatic records to correlate microbial shifts with long-term ecological changes. This multi-proxy approach, grounded in extensive palaeolimnological research at Lake Montcortès, provides a robust framework to assess long-term oxygen variability, microbial community evolution, and their influence on ecosystem resilience and transformation.

2. Materials and methods

2.1. Study site

Lake Montcortès (42°19′50″N, 0°59′41″E) is a karstic lake in the South Pyrenean Central Unit at 1027 m a.s.l. (Fig. S1). It has a surface area of 0.14 km^2, a maximum depth of 32 m, and a 1.4 km^2 catchment. The lake is fed by an ephemeral inlet, while groundwater inflows enriched in carbonates and sulfates dominate its hydrology (Corella et al., 2019). The catchment lies in a climatic transition zone between Mediterranean lowlands and montane forests dominated by oaks and conifers. Surrounding land use includes pastures, meadows, croplands, and littoral vegetation (Rull and Vegas-Vilarrúbia, 2024). The lake is located in the Baix Pallars municipality, which has about 344 residents, only 21 of whom live near the shore (IDESCAT, 2025). Historically, it has been an important water source for nearby villages and farmhouses, reflecting long-term human occupation (Rull and Vegas-Vilarrúbia, 2024; Rull et al., 2022).

Lake Montcortès exhibits a predominantly meromictic regime with occasional holomixis (Vegas-Vilarrúbia et al., 2018, 2020), favouring the formation of annual varves. Seasonal calcite sedimentation, driven by primary productivity, is temperature-dependent (Trapote et al., 2019). The lake is oligo-mesotrophic, with a stable thermocline at 6–10 m persisting through late summer. Phytoplankton biovolumes exceed 6×10^6 μm^3 mL^{-1} , dominated by Bacillariophytes and Chlorophytes during spring and summer blooms (Vegas-Vilarrúbia et al., 2020; Trapote et al., 2019).

2.2. Coring, dating, geochemical (XRF) analyses, and lake volume calculations

Cores containing varved sediment records and Fe/Mn ratios obtained by X-ray fluorescence (XRF) were used as sedimentary proxies of hypoxia and redox dynamics to reconstruct the volume of hypoxic bottom water in Lake Montcortès. A method adapted to the lake's geomorphological, stratigraphic, and geochemical characteristics, based on Jenny et al. (2013), was applied for this purpose.

The geographic position of the coring sites in Lake Montcortès was determined using a detailed bathymetric model derived from a high-resolution sonar and DGPS survey (Corella et al., 2019). This model accurately represents lake-bottom topography and, together with preliminary core images showing transitions from littoral to distal sedimentary environments, enabled the identification of the approximate oxic–anoxic boundary. Based on unpublished monthly dissolved-oxygen profiles (2014–2016), this boundary was estimated to occur at depths shallower than 20 m.

Water volumes were calculated from the bathymetric model using the Cut/Fill algorithm in ArcGIS 3D Analyst, which quantifies the space between the lake bed and a reference plane. For methodological details and the computational formula, see Supplementary Methods (Section S1).

Cores were subsequently retrieved with a UWITEC gravity corer (Table S1) and sectioned in the laboratory to verify the presence and preservation of sediment varves.

To assess variations in the oxic-anoxic conditions in the sediments, high-resolution XRF core scanning was conducted at 0.2 mm resolution using an AVAATECH core scanner (2000 A, 10–30 kV, 20–50 s per measurement) on dated cores MONT-0713-G03, MONT-0119–19, MONT-0119–22, and TR4. Subdecadal time series for iron (Fe) and manganese (Mn) were generated and subsequently averaged to produce annual values. Manganese oxides, which are more readily reduced than iron oxides, tend to dissolve first under reducing conditions, increasing the Fe/Mn ratio and signaling the onset of anoxia (Boyle, 2001). However, if anoxia becomes permanent (meromixis), the Fe/Mn ratio may decrease due to the depletion of Mn and Fe oxides (Davies et al., 2015). Notably, terrestrial Fe inputs can compromise the reliability of the

Fe/Mn ratio as a redox indicator. In this study, an ~50 cm turbidite layer (1845–1900 CE) was present in all targeted cores (Figs. S3, S4), and a clastic layer dating to ~1750 CE in TR4 skewed the Fe/Mn ratios (see Corella et al., 2011 for more details). These layers were therefore excluded from the XRF analysis.

Chronological control for the studied sequence was established using the six-century age–depth model of Corella et al. (2014), (2011), which was based on varve counting and $^{210}Pb/^{14}C$ dating of Montcortès cores MON12–3A-1G and MON12–2A-1G. This model was transferred to cores MONT-0713-G03, MONT-0119–11, MONT-0119–19, MONT-0119–22, and TR4 via stratigraphic correlation, identifying 96 marker horizons.

2.3. Analysis of sedimentary microbial communities

Core MONT-0119–11 was transported to the laboratory and stored frozen at −20 °C. Eighty-eight sediment samples were collected at 0.5–1 cm intervals, processed in a sterile clean lab, and stored at −20 °C. Instruments were sterilized with 10 % bleach and 70 % ethanol. Approximately 1 cm^3 of sediment was taken per depth, placed in sterile 2 mL tubes, weighed, labelled, and frozen at −20 °C until DNA extraction. DNA was extracted from each sample using the FastDNA Spin Kit for Soil (MP Biomedical) according to the manufacturer's instructions. The quality and concentration of DNA in the extracts were measured with a NanoDrop 2000 spectrophotometer (Thermo Fisher Scientific; Wilmington, DE, USA) by measuring A_{260}/A_{230} and A_{260}/A_{280} absorbance ratios and a Qubit 2.0 fluorometer (Life Technologies; Carlsbad, CA, USA), respectively.

High-throughput multiplexed *16S rRNA* gene sequencing was carried out using the primer pair 515 f/806r (Caporaso et al., 2011, Apprill et al., 2015, Parada et al., 2016), which target the V4 region of the *16S rRNA* gene complemented with Illumina adapters and sample specific barcodes. Sequencing was performed at the Sequencing and Genotyping Unit of the Genomic Facility/SGIker of the University of the Basque Country (Leioa, Spain). To barcode samples, a multiplex identifier Golay barcode was attached to the forward primer. Indexing and amplification were achieved in a single PCR reaction. The thermocycler profile consisted of an initial denaturation step at 94 °C for 3 min; 35 cycles of 94 °C for 45 s, 50 °C for 60 s, and 72 °C for 90 s with a final elongation step at 72 °C for 10 min. Equimolar concentrations of samples were pooled and purified using CleanNGS beads (CleanNA). Paired-end sequencing was then performed with a MiSeq reagent kit v2 of 500 cycles according to the manufacturer's guidelines on an Illumina MiSeq. Raw sequence data were deposited in NCBI SRA under the project ID PRJNA869917 .

Sequence read demultiplexing was performed in QIIME2 release 2020.8 (Bolyen et al., 2019). The Dada2 algorithm implemented in QIIME2 was used to denoise, merge paired reads, filter chim eras, dereplicate, and cluster sequences into amplicon sequence variants (ASVs). The feature-classifier script implemented in QIIME2 was employed for the taxonomic assignment using the SILVA reference database (release 138, pre-trained naive Bayes classifier from the 515 f/806r region).

The resulting ASV table and taxonomy were imported into R v4.1.2 (R Core Team, 2021). We filtered the dataset to retain those ASVs with a minimal proportional abundance in a sample of 0.1 % and a prevalence for each feature in all samples of 0.1 % with the *CoDaSeq* package v 0.99.7 (Gloor et al., 2017). We estimated the zero count values with the *Compositions* package v 1.5.0–4 (Palarea-Albaladejo and Martín--Fernández, 2015) before the centered log-ratio transformation of the data was performed to address the compositional nature and sparsity of microbiome datasets (Gloor et al., 2017). We further gathered ASVs into the most abundant orders per sample with the function *top_taxa* from the *fantaxtic* package v0.2.1 (Teunisse, 2022). Since some samples were assigned to the same year, the mean ASV abundances for these samples were calculated, resulting in a total of 73 samples for subsequent analyses.

2.4. Environmental descriptors

We evaluated potential microbial responses to climatic and environmental changes in the lake and its catchment since 1500 CE by applying a suite of well-established biotic and abiotic proxies. These proxy data were derived from previous studies conducted at Lake Montcortès and across the Pyrenees during the same time frame (Table 1). To align biological, climatic, and environmental events recorded in separate sediment cores, we employed chronostratigraphic correlation, biostratigraphy, and the identification of event markers, using available age models, subfossil assemblages, and distinct geochemical or sedimentary signatures shared among the records.

2.5. Statistical analyses

2.5.1. Alpha and beta diversity of filtered microbial communities

The compositions of the most abundant ASVs in the sediment core across centuries were compared using taxonomy bar plots constructed in the R software (R Development Core Team, 2011) with the *phyloseq* v. 1.46.0 and *qiime2R* v 0.99.6 packages (Bisanz, 2018;McMurdie & Holmes, 2013). We also calculated the Shannon index in R using the

Table 1
Environmental descriptors. Information sources: [1] Vegas-Vilarrúbia et al. (2022); [2] Dorado-Liñan et al. (2012); [3] Rull & Vegas-Vilarrúbia (2024); [4] Montoya et al. (2022), [5]: Corella et al. (2014), (2011); [6] Vegas-Vilarrubia et al. (2018); [7] Trapote et al. (2019).

Proxy type	Variable	Related process	References
Calcite varve-thickness (mm)	Precipitation	Estimations of mean autumn precipitation in Montcortès.	[1]
Tree rings thickness (mm)	Temperature anomalies	Estimations of mean autumn temperatures in the Pyrenees.	[2]
Pollen grains (%)	*Cannabis* (Ca) Tree pollen	Cultivation and retting. Vegetation.	[3,7]
Fungal spores (%)	*Sporormiella* (sp.), *Glomus*	Livestock. Soil erosion.	[4]
Charcoal particles (%)	Derived from burning of wood	Regional fires (≤150 μm particle size).	[3,7]
Elemental composition XRF, counts per second (cps)	Manganese (Mn) Silica (Si) Calcium (Ca) Bromine (Br)	Detrital input from catchment, redox conditions. Coarse silt and sand from catchment. Endogenic calcite, detrital carbonates from catchment. Higher productivity or organics	[5, 6]
Elemental composition ratios	S/Ti S/Fe Fe/Mn Fe/Ti	Sulfur mobilization in sediment. Pyrite (Fe–S) formation in sediment. Redox indicator in sediment. Iron mobilization in sediment	[6]
Pigments	Total Chl a Oscillaxanthin (Cyanobacteria) Aphanizophyll (N_2- fixers) Isorenieratene (Chlorobiaceae) Okenone (Chromatiaceae)	General primary production warming-driven photosynthesis Nitrogen fixation Anoxygenic photosynthetic bacteria indicating photic anoxia. Anoxygenic photosynthetic bacteria indicating photic anoxia.	[6.7]

vegan package v. 2.6–8 (Oksanen et al., 2020) to the evaluate species diversity of the most

abundant orders. One-way analysis of variance (ANOVA) using the *ANOVA* function of the *car* package v. 3.1–7 (Fox et al., 2021) was used to detect differences in diversity across centuries, followed by pairwise comparisons.

For beta diversity, hierarchical clustering was performed using the Aitchison distance of CLR-transformed ASV values with the *hclust* function from the R package *stats* v. 4.4.1 and the function *dendro_data* from the e *ggdendro* v. 0.2.0 packag (De Vries and Ripley, 2024), to assess sample grouping across centuries.

Significant differences in beta-diversity across centuries were assessed using one-way permutational multivariate analysis of variance (PERMANOVA) using the *adonis2* function of the *vegan* package (Oksanen et al., 2020), with a factor of century. Pairwise comparisons were subsequently conducted using the *RVAideMemoire* package v. 0.9–87–3 (Hervé, 2021).

2.5.2. Percentage diagram of the stratigraphically constrained ASVs

To reflect major changes in bacterial ASVs, the results of the *16S rRNA* gene analysis were plotted in a stratigraphically constrained percentage diagram using Psimpoll 4.27 (Bennett, 1992), in which zonation was determined using the optimal splitting by information content and broken-stick methods (Bennett,(1996). Other statistical analyses were conducted with PAST 4.12 (Hammer et al., 2001).

2.5.3. Multivariate analyses

Bacterial community composition was analyzed in relation to environmental variables using multivariate ordination techniques. A detrended correspondence analysis (DCA; Hill and Gauch, 1980) indicated a gradient length exceeding 3 SD units, suggesting a unimodal response of ASV composition to environmental gradients. Consequently, a canonical correspondence analysis (CCA; ter Braak, 1986) was performed, following the 2.5–3 SD criterion (ter Braak and Prentice, 1988; Lepš and Šmilauer, 2003), using ASV data and standardized environmental variables. To assess the relative contributions of anthropogenic and climatic factors, a variance partitioning analysis (VPA) was carried out with the *varpart* function in the *vegan* package (Oksanen et al., 2020) on the Hellinger-transformed ASV matrix, using Cannabis influx and temperature as explanatory variables.

3. Results

3.1. Variations in the volume of anoxic water

All cores containing non-varved sediments were extracted from locations within approximately 35 m of the shoreline, at water depths no greater than 16 m (Fig. S2). Core TR3, retrieved from a depth of 15.6 m, was the first along the depth gradient to exhibit varve strips in its stratigraphic profile. Two varve intervals were identified within the silt-clay unit (0–55 cm): one between 25–30 cm depth and the other between 40–45 cm depth (Fig. S5). Lithostratigraphic correlation linked the lower boundary of Unit I in TR3 (55 cm) to the upper boundary of Unit III in TR4 (14 cm), corresponding to sediments deposited around 1942 CE. These findings suggest that the varves observed in TR3 formed after 1942, reflecting two exceptional instances where anoxic water from the monimolimnion rose to a depth of 15–16 meters. In contrast, varves in other cores were found at greater depths, indicating that such upward displacements of the oxic-anoxic boundary were rare. Based on TR3's depth of 15.6 m, the estimated volume of anoxic water during these events was approximately 665,513 m^3 . Overall, the results suggest that fluctuations in the oxic-anoxic boundary typically remained below 15–16 m since 1500 CE, as continuous varves were exclusively observed in cores retrieved from deeper locations.

The subsequent analysis focused on estimating the annual anoxic water volume (VAW) using Fe/Mn ratios in varved cores MONT-0713-G03, MONT-0119–22, MONT-0119–19, and TR4 (Fig. 1; see Supplementary Material, Section S2, for additional details). As previously noted, the Fe/Mn ratio is a proxy for redox conditions in lacustrine sediments. To better identify transitions between oxic and anoxic states, we examined the Fe/Mn time series to determine threshold values specific to each core. This involved analysing Fe/Mn distributions using central tendency, range, variability, and outliers; boxplots for each core visualized these patterns effectively. (Fig. S6). The boxes were defined by the 25th and 75th percentiles, encompassing the middle 50 % of the data values. We interpreted Fe/Mn values within this interquartile range (IQR) as representing redox conditions, likely reflecting seasonal or short-term shifts in bottom-water oxygenation. Whiskers, extending beyond the box, indicate the spread of Fe/Mn values within 1.5 times the IQR. Fe/Mn values below the 25th percentile were associated with supra-annual anoxia dynamics, which likely occurred during meromictic years when significant Fe oxide reduction occurs without annual replenishment. Conversely, Fe/Mn values between the 75th percentile and the upper whisker likely reflect increased Fe precipitation resulting from oxygenation of the monimolimnion. This condition is more common in the shallower zones of Lake Montcortès or during years when full turnover of the water column occurs. Extreme Fe/Mn values beyond the upper whisker were interpreted as episodic inputs of eroded iron oxides from the catchment. These outliers were excluded from further analysis. To delineate the data needed to estimate temporal variations in the anoxic volume of water (monimolimnion), we used the 75th percentile Fe/Mn ratio of each core as the threshold for distinguishing between oxic and anoxic conditions in the monimolimnion at each sediment core location.

With these thresholds, the next step was to estimate the VAW values on a yearly basis since 1500 CE. To this end, the mapped cores were chronologically correlated, so that the respective Fe/Mn thresholds could be compared on a year-by-year basis. Therefore, for each particular year, the shallowest coring point with values lower than the 75th

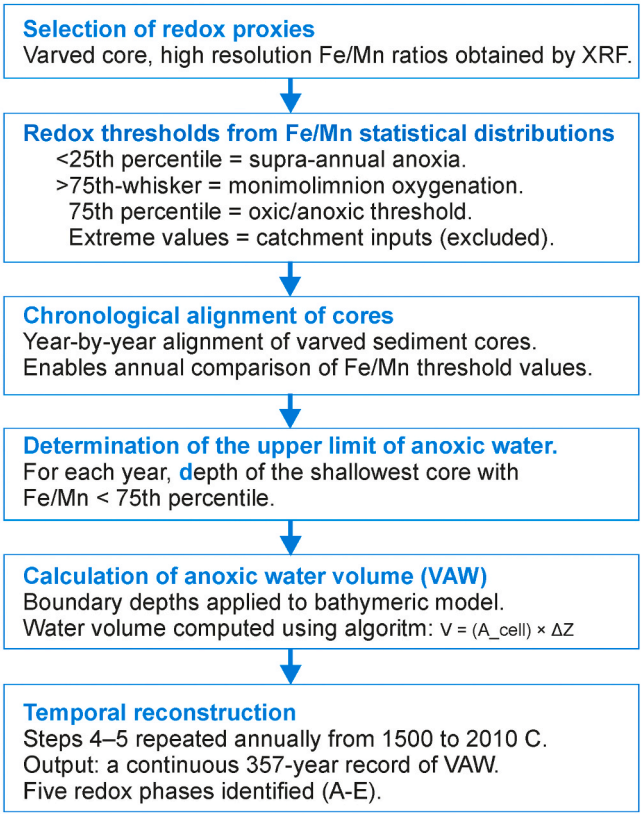

Fig. 1. Lake Montcortès anoxic water volume reconstruction flowchart.

percentile was chosen, and its water depth (i.e., the vertical distance from the lakebed) was taken to estimate the maximum level reached that year by the anoxic water rising from the bottom. For example, for the year 1600 CE, cores MONT-0119–22 (18 m) and MONT-0119–19 (16.2 m) showed Fe/Mn values exceeding the 75th percentile and indicated significant oxic conditions at these points, whereas the Fe/Mn ratios at TR4 (20 m) and MONT-0713-G03 (28.6 m) were lower and consistent with oxygen deficiency.

These results indicate that the anoxic water ascended from the bottom to at least 20 m (TR4) from the lake's surface but remained below 18 m, thus indicating that the targeted VAW was somewhere between 396,608 m^3 (TR4) and 521,124 m^3 (MONT-0119–19). Since the exact minimum depth (maximum VAW) reached by the anoxic water could not be determined, we arbitrarily took the depth of the shallowest location showing anoxia, in this case TR4, for VAW assessments. This procedure was repeated annually from 1500 to 2010 CE, yielding a continuous 357-year VAW time series (Fig. 2). Overall, bottom anoxic conditions were present every year seasonally. According to the results, the VAW of the lake fluctuated between 390,500 m^3 and 609,100 m^3 with an average 550,000 m^3 (SE ± 351 m^3) from1500 to 2011 CE. This represents 16.0–25 % of the total volume of lake water. The changes in VAW over time broadly followed five distinct patterns (A-E), each reflecting different meromixis durations and oxygenation dynamics within the lake's monimolimnion (Fig. 2). The results of a non-parametric One-Way Kruskal-Wallis test (H =76,95 $p < 0.0001$) indicated that water volume differed significantly among the five groups.

The estimated average VAW value of the preindustrial period (1500–1750 CE) was 545,560 m^3 with a coefficient of variation of 14.4. Interestingly, the average VAW of the postindustrial period (1905–2010 CE) increased to 558,692 m^3 and remained quite stable, with a coefficient of variation of only 2.62. A greater persistence of the VAW occurred from 1937 onwards. This was confirmed by the instrumental records of DO (Hydrolab multiparametric DS5 probe) between 2013 and 2020, when the maximum VAW reached 1018,400 m^3 (41.7 %) and anoxia ascended to 11.5 m from the lake surface. We subsequently explored potential correlations between VAW minima and climatic conditions since 1500 CE (Fig. 2).

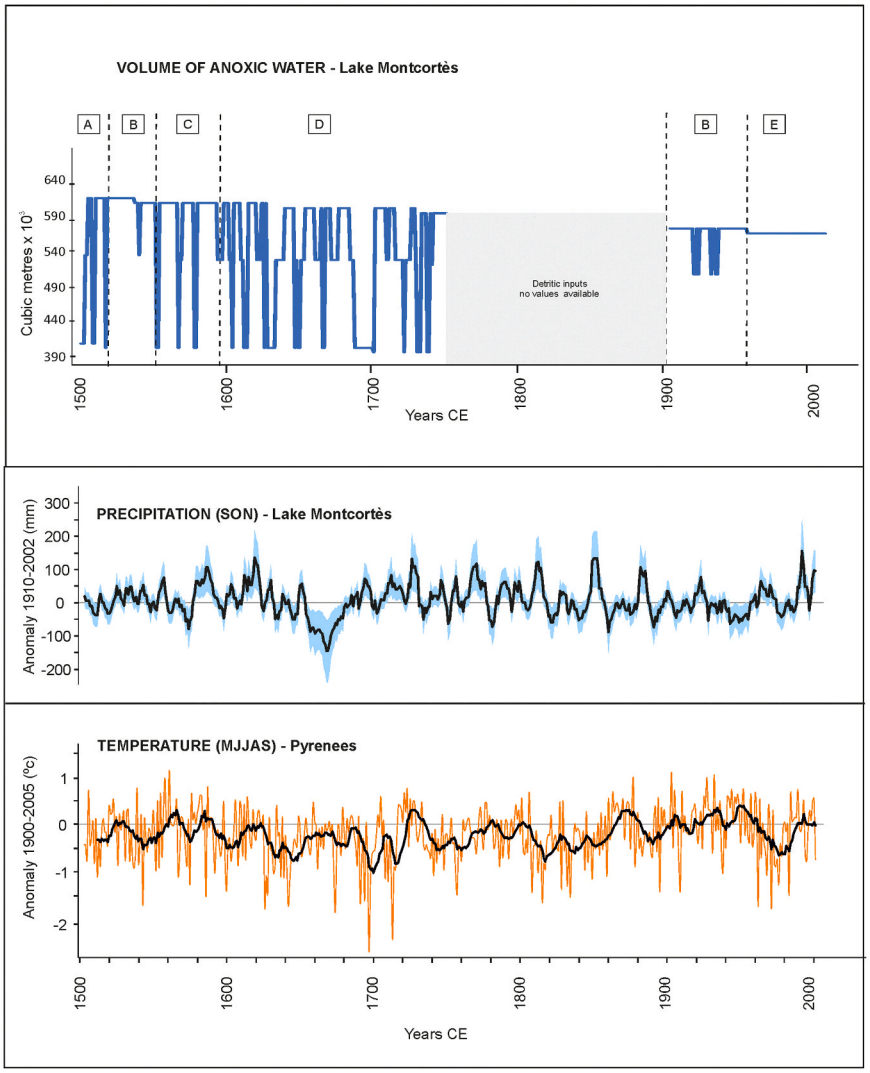

Fig. 2. Top panel: Estimated maximum annual volume of anoxic water (VAW) in Lake Montcortès from 1500 to 2010 CE. Periods are marked: A (pre-1600 CE), persistent meromixis with occasional deep oxygenation; B (1600–1700 CE), frequent deep oxygenation, instability, and marked fluctuations in VAW; C (1700–1900 CE), transitional phase with episodic mixing, note the data gap (~1750–1900 CE) caused by turbiditic/clastic inputs; D (1900–2000 CE), relative stabilization with reduced deep-water oxygenation; E (post-2000 CE), strengthened meromixis with minimal seasonal mixing.
(a) Middle panel: Autumn (SON) precipitation anomalies for Lake Montcortès (adapted from Vegas-Vilarrúbia et al., 2022). (b) Bottom panel: Summer (MJJAS) temperature anomalies in the Pyrenees since 1500 CE (adapted from Dorado-Liñán et al., 2012).

3.2. Composition of sedimentary bacterial communities

After denoising and quality filtering the sequence libraries, a total of 5218,065 reads were obtained across the 88 samples, revealing a range of reads per sample spanning from 2166 to 102,814. Sample 78 was excluded from the analysis because of its poor read count (2166). The amplicon sequence variant (ASV) accumulation curves reached a plateau phase for all samples (Fig. S7), indicating that we captured the majority of the sample richness. The final ASV table encompassed a total of 20,170 ASVs, 1694 of which were retained across the 87 samples after filtration by 0.1 % abundance. When we averaged those samples assigned to the same year and filtered the dataset by the most abundant orders, we ultimately kept 110 ASVs (0.5 % of the total ASVs) across 73 samples, representing 56 % of the total abundance. Analysis of the sediment bacterial communities in the different sediment zones (i.e., centuries) revealed clear variation in composition (Fig. S8). Over the span of centuries, the prevalent order was Campylobacterales (averaging 28 %). In the XVIth, XVIIth, and XXth centuries, the second-most dominant order was Burkholderiales (13 %, 18 %, and 12 % respectively), whereas Bacillales occupied the second dominant position in the XVIIIth and XIXth centuries (12 % and 13 %, respectively).

Diversity analysis revealed significant differences in Shannon diversity (H) across centuries (Fig. 3). For the Shannon diversity, the Type III ANOVA revealed a significant effect of century ($F = 6.825$, $p = 0.0001$), with notable fluctuations in AVS species diversity over time, particularly in the XIXth century. The high intercept F-value ($F = 4573.3$, $p < 2.2e^{-16}$) represented the overall diversity level, whereas the century effect highlighted significant deviations from this baseline.

Beta diversity analysis further supported the previous findings, with PERMANOVA showing a significant effect of century (p value = 0.001), and all pairwise comparisons yielded p values < 0.003. The resulting dendrogram revealed clear clustering of samples by century, reflecting temporal shifts in species turnover (Fig. S9).

3.3. Variation in microbial ASVs along the stratigraphic record

Bacterial community composition across the sediment sequence spanning the last five centuries was analysed using the relative abundances of ASVs at the order level, including only taxa ≥ 0.1 % relative abundance. Results are shown as a percentage diagram (Fig. 4), illustrating temporal changes and succession in bacterial orders since 1500 CE. The analysis delineated seven statistically distinct zones, each representing major shifts in community structure through time.

3.3.1. Zone M-1 (14 samples): depth 970–890 mm, circa 1512–1636 CE

Zone M1 was dominated by ASVs assigned to the orders Campylobacterales, Burkholderiales, and Bacillales, followed by Spirochaetales, Caldisericales, Caldatribacteriota (JS1 unclassified), and Dehalococcoidia (MSBL5). Burkholderiales increased markedly after 1600 CE but declined at the transition to zone M2.

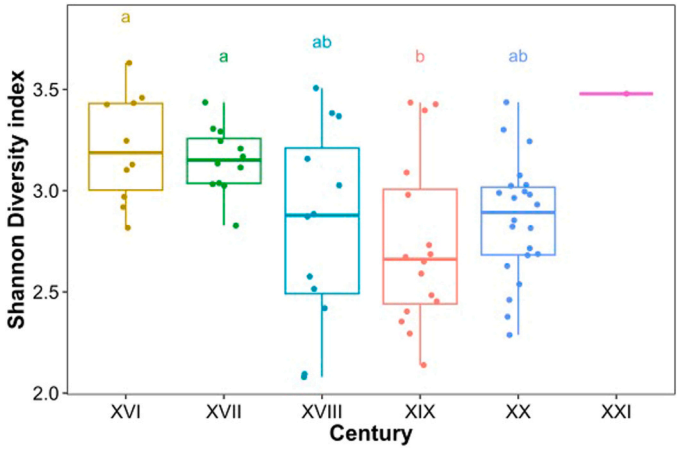

Fig. 3. Shannon-Wiener diversity index across various centuries.

3.3.2. Zone M-2 (12 samples): depth 885–820 mm, circa 1637–1719 CE

ASVs assigned to Burkholderiales declined sharply, reaching their lowest levels between 1690 and 1700 CE, coinciding with a marked decrease in Campylobacterales. In contrast, Desulfomonadales, Thermodesulfovibrionia, Dehalococcoidia (MSBL5), and Phycisphaerae (MSBL9) peaked during this interval, with the latter two reaching their maximum abundances for the entire record. Pseudomonadales also became increasingly prominent during this period.

3.3.3. Zone M-3 (1 sample): 815–805 mm, circa 1720–1737 CE

This brief 26-year period was characterized by a abrupt increase in Bacillales, which reached their highest abundance of the entire record by 1720 CE, while Campylobacterales and Burkholderiales declined markedly. ASVs associated with JS1 and Spirochaetales decreased from the onset of this zone, while those affiliated with Rhizobiales and Nitrososphaerales peaked early around 1730 CE. The sharp peak of Bacillales peak near 1720 CE, represented by a single sample, should be interpreted cautiously. Additional context is provided in Section 4.

3.3.4. Zone M-4 (15 samples): depth 800–625 mm, circa 1738–1840 CE

This zone is markd by a recovery of Campylobacterales and a sharp decline in Bacillales. From this point onwards, extending to the end of the record (zone M-7), both orders show consistently opposing trends. ASVs assigned to Burkholderiales, Pseudomonadales, MSBL5, and Woesearchaeales also display moderate recoveries.

3.3.5. Zone M-5 (13 samples): depth 620–205 mm, circa 1841–1912 CE

Campylobacterales sharply declined between 1850 and 1870, while Bacillales peaked around the same time, and Burkholderiales increased gradually throughout this zone. Caldisericales and Pseudomonadales showed brief peaks at the start of the zone, then declined to minimum levels maintained through zones M6 and M7 to the present. Zone M5 also featured minor maxima of Rhizobiales, Anaerolineales, Desulfomonadales, and unclassified ASVs within the candidate phylum Zixiibacteriota.

3.3.6. Zone M-6 (10 samples): depth 195–140 mm, circa 1912–1963

This zone is characterized by fluctuations in Burkholderiales, a sharp decline in Bacillales, and the recovery and stabilization of Campylobacterales. It also shows an increase in previously less abundant taxa, including Steroidobacterales, MSBL5, and several groups of sedimentary archaea such as Marine Benthic Group D and DHVEG-1.

3.3.7. Zone M-7 (7 samples): depth of 135–85 mm, circa 1963–2006

In this surficial zone, Campylobacterales decreased slightly, while Burkholderiales gained prominence and Bacillales nearly disappeared. Verrucomicrobiales reached notable relative abundances for the first time, and Thermodesulfovibrionia and Desulfomonilales also increased.

3.4. Multivariate analysis

Building on previous results, we examined relationships between bacterial ASV composition and environmental variables. A preliminary DCA showed a gradient length exceeding three standard deviation units of ASV turnover, indicating a unimodal response. Consequently, a CCA was selected as the most appropriate ordination method. The CCA explained a substantial portion of the total variance in bacterial community composition (Table S2). Axis 1 (27.9 % of constrained variance; 14.2 % of total inertia) represents the main ecological gradient dominated by redox-sensitive variables. Axis 2 (20.9 % of constrained variance; 10.6 % of total inertia) is primarily associated with *Cannabis* influx and, to a lesser extent, with proxies of primary production and

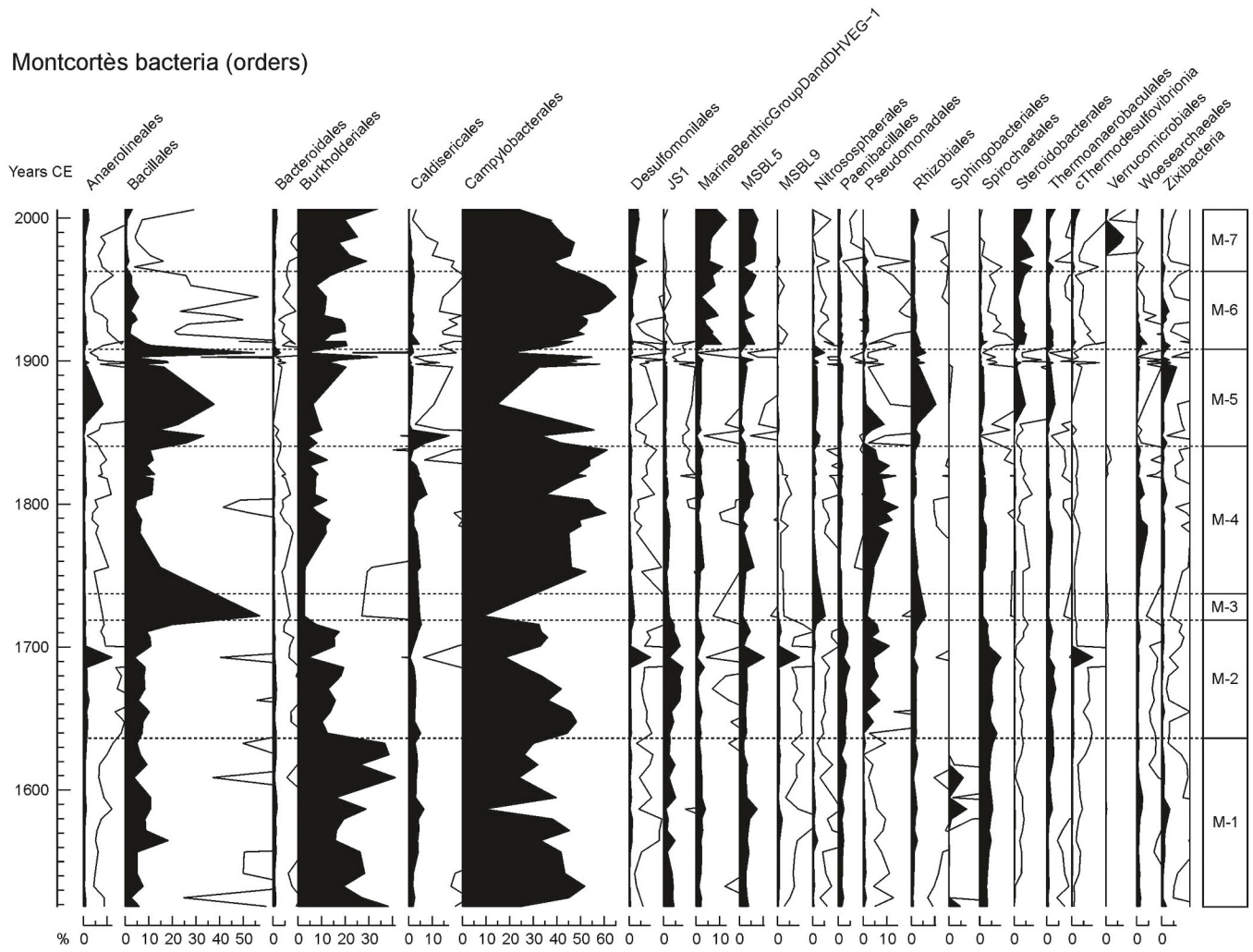

Fig. 4. Psimpoll percentage diagram showing temporal variations in bacterial orders with relative abundances ≥ 0.1 %. Solid lines represent values magnified × 10. Dashed lines mark seven statistically distinct zones (M1–M7) defined using the OSIC and broken-stick methods (Bennett, 1992, 1996). The left axis shows estimated ages based on the age model of core MONT-119–11 (see Supplementary Fig. S2).

temperature. Together, the first two axes explain 48.9 % of the constrained variance (≈25 % of total inertia), capturing the dominant environmental and temporal gradients influencing bacterial community structure over the last five centuries.

The ordination of sample scores by century (Fig. 5) displays a counter-clockwise chronological pattern from the sixteenth to the twenty-first century. Samples from the sixteenth to seventeenth centuries plot on the right side of the diagram, near Mn, Si, and charcoal influx. Eighteenth–nineteenth-century samples shift upward toward the *Cannabis* and Coprophile vectors, while twentieth–twenty-first-century samples cluster on the left, associated with chlorophyll-related proxies and temperature.

The ordination of bacterial response variables (Fig. 6) reveals compositional changes along these gradients, with considerable dispersion. Acidobacteriota, Nitrospirae, and Bacillales are linked to oxidized, mineral-rich conditions. Campylobacterales and Pseudomonadales increase with *Cannabis* influx and organic matter loading, whereas Desulfobacterota, Chlorobiae, and Burkholderiales prevail under reducing, organic-rich conditions during later, eutrophic phases. Overall, the CCA shows consistent temporal and environmental structuring of bacterial communities along redox and anthropogenic gradients.

4. Discussion

4.1. Dynamics of microbial communities, oxygenation phases and environmental drivers

The structural and functional dynamics of bacterial communities in Lake Montcortès reflect complex interactions with oxygenation patterns, environmental factors, and indirectly, climate. We present a chronological analysis of bacterial community shifts in relation to these drivers over the past 500 years. Despite the acquisition of well-resolved and robust taxonomic patterns across all sediment zones analyzed, the functional interpretations derived from these data remain inherently inferential, as the 16S rRNA gene represents a limited proxy for functional profiling (Matchado et al., 2024). Although several bioinformatic tools are available to infer functional information from 16S rRNA gene amplicon sequence datasets (see review by Djemiel, 2022), these approaches depend on the availability of reference genomes and may introduce bias, particularly when characterizing ancient microbial communities in deep sediment cores. Accordingly, as the present analysis is based solely on the taxonomic assignment of 16S rRNA gene sequences, the following results should be regarded as indicative of the potential presence of the metabolic groups discussed, and therefore interpreted with appropriate caution.

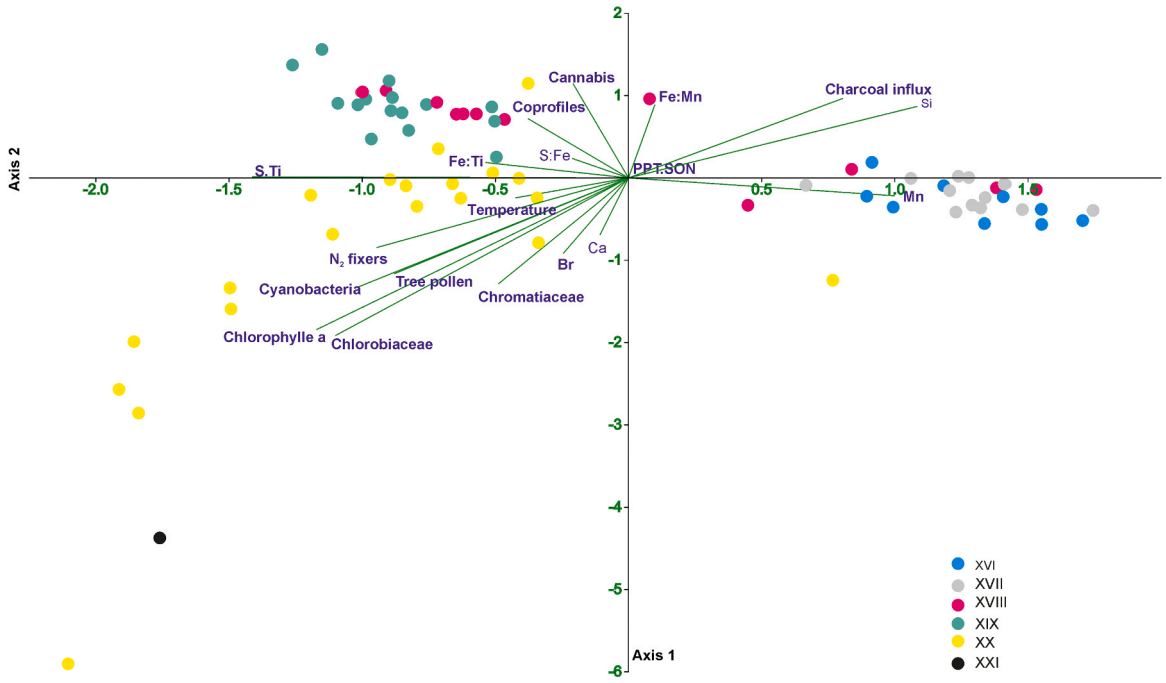

Fig. 5. Canonical Correspondence Analysis (CCA) biplot based on ASV abundance data without replacement. CCA of samples, where each dot represents a filtered bacterial community, color-coded according to the sampling date. Green vectors indicate environmental variables.

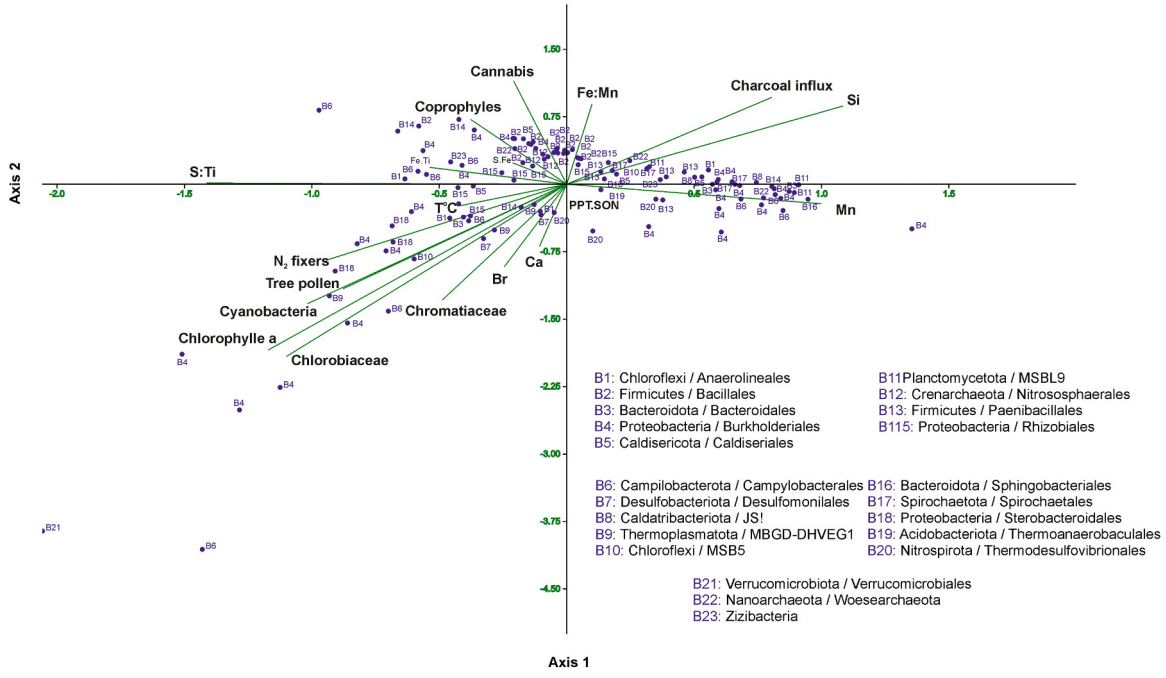

Fig. 6. Canonical Correspondence Analysis (CCA) biplot based on ASV abundance data without replacement. Each dot represents a bacterial ASV labeled by its taxonomic group (B1–B23). Green vectors indicate environmental explanatory variables influencing community composition.

4.1.1. Early anoxia, episodic oxygenation and the onset of Cannabis retting (XVIth and XVIIth centuries)

In Zone M1 (1512–1636 CE), microbial communities thrived under dynamic oxygenation patterns transitioning from mostly stratified conditions to a progressive weakening of meromictic stability, possibly due to external factors such as shifting precipitation or changes in inflows. The strong manganese signal in the CCA is probably caused by redox-driven internal changes, which are reinforced with clastic inputs from catchment erosion processes (Corella et al., 2011). Notably, the cultivation of Cannabis and retting activities began shortly after 1550 CE (Rull and Vegas-Vilarrúbia, 2024). Early in hemp water retting, microbes degrade pectins and hemicelluloses and release simple sugars with little impact on dissolved oxygen. Later, cellulolytic bacteria break down cellulose, slowing carbon release and depleting oxygen, altering water chemistry (Fu et al., 2011). These biological processes are driven mainly by diverse bacterial groups affiliated with the phyla Pseudomonadota, Chloroflexota, Bacteroidota, Actinomycetota, Planctomycetota and Bacillota (formerly known as Firmicutes) (Tamburini et al.,

2015; Iwańska et al., 2022; Bou Orm et al., 2024).

A previous study in Lake Montcortès identified members of Bacillota (e.g., Bacillus, Clostridium) and various genera within Pseudomonadota (e.g., Massilia, Rhizobium, Pseudomonas, Escherichia, Methylobacterium, Rhodobacter) in Cannabis fibres (Rull et al., 2022). In the present work, additional bacterial groups not directly associated with pectinolytic metabolism were detected. Members of Campylobacterales emerged as prominent chemolithoautotrophs inhabiting sulfidic redoxclines, a pattern consistent with observations from both freshwater and marine systems (Lin et al., 2006; Glaubitz et al., 2010; Grote et al., 2008; Noguerola et al., 2015). Similarly, taxa affiliated with Spirochaetales, Dehalococcoidia, Caldatribacteriota, and Caldisericales increased during prolonged anoxia, supporting their role in anaerobic organic matter degradation (Martínez et al., 2019; Rodríguez et al., 2025; Yu et al., 2023). Furthermore, the enrichment of facultative anaerobes such as Massilia (Burkholderiales) and Bacillus (Bacillales) under fluctuating redox conditions suggests that these taxa benefited from labile organic substrates generated during rapid hemp stalk decomposition (Bleuze et al., 2020).

4.1.2. Frequent mixing events, intensification of Cannabis retting, and sulfate reduction (XVIIth and XVIIIth centuries)

Zone M2 (ca. 1637–1720 CE) was characterized by frequent deep-water oxygenation (B), coinciding with the coldest and driest phase of the Little Ice Age (ca. 1300–1850 CE) in the Central Pyrenees (Fig. 2). Cooling and drought likely weakened stratification and reduced nutrient inputs, promoting recurrent mixing. Despite this, microbial data show the proliferation of sulfate-reducing bacteria (Desulfomonadales, Thermodesulfovibrionales), indicating anaerobic organic matter oxidation in anoxic bottom waters and sediments. Simultaneously, increased Pseudomonadales suggest enhanced fermentative processes, probably linked to retting byproducts. Though seemingly paradoxical with greater oxygenation, intensified hemp retting around 1720 CE (Rull and Vegas-Vilarrúbia, 2024) likely raised oxygen demand. Retting added labile, cellulosic organic matter, enriching the accumulated load since ~1550 CE and rapidly depleting oxygen despite mixing. Thus, localized anoxia supported sulfate-reducing and fermentative bacteria, reflecting a dynamic interplay between physical processes and biogeochemical feedbacks under climatic and anthropogenic pressures.

4.1.3. Episodic sediment influx, nutrient pulses and the influence of the retting (XVIIIth century)

In Zone M3 (1720–1737 CE), episodic oxygenation events in the post-LIA period continued, but were driven by increased rainfall and rising temperatures (Fig. 2). Enhanced detrital influx from the catchment (Si, Mn) and charcoal deposition from regional fires likely disrupted stratification and sediment layers, and heightened water turbidity. Additionally, Cannabis retting activities peaked, incorporating substantial inputs of plant organic matter and nutrients into the lake. Notably, the combined effects of these factors may have created favourable conditions for the germination of bacterial spores, which might explain the abrupt increase in Bacillales observed in this period, and the concurrent drecrease in the relative abundances of Campylobacterales and Burkholderiales. The simultaneous presence of other facultative anaerobes and fermentative bacterial groups is also indicative of conditions favouring anaerobic metabolism. Moreover, the modest increase in microaerophilic ammonia-oxidizing archaea (i.e., Nitrososphaerales) and N_2-fixing Rhizobiales also suggests oxygen-limiting conditions. This shift reflects accelerated nitrogen turnover, which is likely driven by enhanced organic matter inputs and redox fluctuations, further influencing ecosystem biogeochemistry.

4.1.4. Decline of retting, sulfate reduction and onset of euxinic conditions (XVIIIth and XIXth centuries)

Until approximately 1750, the frequency of oxygenation and VAW fluctuations remained similar to those in zone B. Between 1738 and 1840 CE (M-4), the microbial community continued to reflect the lasting effects of Cannabis retting. *Desulfomonadales* and *Thermodesulfovibrionales* sustained sulfate reduction, leading to sulfide accumulation of in the bottom water. Under strongly sulfidic (euxinic) conditions, the simultaneous increase in the Fe/Mn and S/Fe ratios likely promoted the formation of iron sulfides such as pyrite (FeS_2) (Davison, 2003; Davies et al., 2015). Indeed, framboidal pyrite crystals have been observed in the sediment of Lake Montcortès (Vegas-Vilarrúbia et al., 2018).

4.1.5. Turbidites and cessation of retting activities (XIXth to early XXth centuries)

From the middle of the XIXth century, climatic conditions in the Pyrenees became unstable and the mean temperature rose (Fig. 2), and the lake gradually transitioned towards intermittent meromixis (Zone C). Between 1841 and 1912 (zone M5), turbiditic deposition of allochthonous clastic and organic material disturbed the sediment profile (Corella et al., 2011), but variations in the Fe/Ti and S/Fe ratios consistently indicate reducing and euxinic conditions over the remaining part of this period. Hemp retting experienced another peak between 1840 and 1870 before being finally abandoned in the first decades of the XXth century (Rull et al., 2022). This resurgence of retting activities might explain the new increase in the relative abundance of Bacillales, Rhizobiales, and Pseudomonadales, along with a coincident decline in Campylobacterales. By the mid-XXth century, the cumulative effect of more than three centuries of hemp fibre degradation had likely transformed the sediment composition and biogeochemical properties of the lake.

4.1.6. Thermal stratification, reforestation, and internal productivity (Late XXth and XXIth centuries)

Between 1913 and 1963 CE (M6), the frequency of lake-mixing years markedly declined, leading to stronger stratification of the water column (D) under the growing influence of global climate warming (IPCC, 2021). Reforestation and reoligotrophication advanced as natural forests regenerated, driven by the abandonment of traditional agriculture and hemp cultivation and widespread migration to industrial areas (Vegas-Vilarrúbia et al., 2018; Rull and Vegas-Vilarrúbia, 2024). Hemp retting had ceased entirely, and the pollen peak recorded during this period derived from extensive hemp crops for paper pulp production hundreds of kilometers to the southwest, as well as likely illegal Cannabis plantations near Montcortès (Rull and Vegas-Vilarrúbia, 2023; Rull et al., 2024). Consequently, hemp fibers were no longer submerged, and aquatic ecological dynamics were unaffected by retting. Organic inputs shifted from pectin- and cellulose-rich retting materials to more diverse, labile sources from the watershed, favoring generalist heterotrophic bacteria. Meanwhile, renewed stratification restored sulfidic redoxclines and promoted microaerophilic chemolithotrophic sulfide oxidizers within Campylobacterales (e.g., *Sulfuricurvum*, *Arcobacter*) and Burkholderiales (e.g., *Thiobacillus*).

4.1.7. Intensification of climate warming and the strengthening of stratification

From 1963–2006 (M7), lake stratification intensified sharply, and prolonged periods of meromictic conditions became the norm (E). Biogenic calcium precipitation and pigment records indicate increased N_2-fixing and non-N_2-fixing Cyanobacteria in the upper oxic layers, alongside blooms of purple and green anoxygenic sulfur bacteria within sulfidic redoxclines (Vegas-Vilarrúbia et al., 2018; Trapote et al., 2019). Despite the consistent occurrence of okenone and isorenieratene in sediments since 1500 CE (Vegas-Vilarrúbia et al., 2018), sequences affiliated with Chromatiaceae and Chlorobiaceae were rare in our datasets (0.01 % and 0.004 %, respectively), indicating a very different preservation rates of both biomarkers. While sedDNA can persist for extended periods under favorable conditions (Carini et al., 2016; Dommain et al., 2020; Ogata et al., 2021), algal and bacterial pigments—particularly carotenoids from green sulfur bacteria—are

generally more stable over geological timescales and are widely used as indicators of photic-zone anoxia (Chen et al., 2001; Koopmans et al., 1996; Mallorquí et al., 2005). However, some studies report no clear decline in the number of SSU rDNA of green sulfur bacteria with sediment age (Boere et al., 2011), suggesting that DNA preservation may sometimes rival that of pigments. Although a detailed assessment of differential biomarkers-DNA preservation of was beyond the scope of this study, concurrent shifts in microbial composition were evident: Bacillales nearly disappeared, while Steroidobacterales, Desulfomonilales, and Thermodesulfovibrionales increased moderately, and aerobic heterotrophs (Verrucomicrobiales) appeared for the first time. While our results are inferential, previous studies have shown that members of Verrucomicrobiales can compete with methanogens for hydrogen and acetate, thus influencing methane cycling in sulfate-rich environments (Chiang et al., 2018).Although our data do not provide direct evidence of methane production, the presence of archaeal methanogens suggests that methanogenic activity in the lake monimolimnion may have been higher than expected (Zhang et al., 2019).This microbial shift likely coincided with the onset of the Great Acceleration (IPCC, 2021)

4.2. Long-term deoxygenation dynamics and resilience of the bacterial community

Previous studies have provided valuable insights into deoxygenation processes associated with eutrophication and/or climate change, typically covering the past few decades to, in some cases, one or two centuries (e.g. Huang et al., 2022; Jane et al., 2021, 2023; Jansen et al., 2024; Jenny et al., 2014; Müller et al., 2012; Zhang et al., 2023; 2025). Building on this foundation, our study extends the temporal perspective by examining a longer-term record from Lake Montcortès. Our results reveal that historical human activities have left a lasting biogeochemical legacy that continues to shape deoxygenation dynamics and contribute to present-day oxygen loss. In addition, recent global warming has intensified thermal stratification and temperature-driven outgassing, further exacerbating deoxygenation. Despite fluctuations in oxygenation and variation in carbon sources, the bacterial community is diverse and remains resilient, maintaining functional stability despite compositional shifts over centuries (Philippot et al., 2021). Anaerobic bacterial processes in anoxic water layers and sediment deplete oxygen and produce reduced metabolic by-products (*e.g.*, sulfide and methane) that accumulate in bottom waters. Several studies indicate that these conditions create a self-reinforcing feedback loop driven by climate warming, oxygen depletion, and microbial activity (Aben et al., 2017; Lewis et al., 2024; Seidel et al., 2022). As temperatures rise, the monimolimnion remains isolated for longer periods, intensifying oxygen depletion and the expansion of anoxia. In turn, anaerobic microbes produce methane and sulfide, which exacerbate greenhouse warming and deepen stratification. The accumulation of sulfide further impedes reoxygenation, trapping lakes in a persistent cycle of deoxygenation. The spread of anoxic water drives biogeochemical change and ecosystem decline, highlighting the need for adaptive management.

Understanding how deoxygenation reshapes microbial communities supports oxygen trend models and informs integrated mitigation strategies in temperate lakes (Rhodes et al., 2017). Hypoxia raises water treatment costs, depresses fisheries and recreational value, and reduces property values. While hypolimnetic oxygenation offers a potential solution, installation and annual operation can be costly (Horne and Faisst, 2022). Persistent low-oxygen conditions also amplify methane emissions, reinforcing climate feedbacks (Beaulieu et al., 2019).

4.3. Long-term deoxygenation trends in context

By combining sedimentary DNA and XRF analyses on varved sediments spanning five centuries, our study extends beyond the typical temporal scope of previous research and offers a complementary long-term perspective on lake deoxygenation and microbial responses, using indicators that differ from those traditionally employed in similar studies—such as chironomid records (Brooks et al., 2001), geochemical ratios and elements (Ojala et al., 2012), or diatom assemblages (Battarbee, 2000). While sedimentary DNA has previously been applied to explore microbial dynamics over both shorter and longer timescales (e.g Monchamp et al., 2019, 2016; Savichtcheva et al., 2015), these studies have primarily focused on community shifts and did not focus on reconstructing extended oxygenation trends. A more closely related methodological example to our study is Lake Tiefer See (Germany), where sedimentary DNA analyses were applied to reconstruct cyanobacterial dynamics across the Holocene, though not with a direct emphasis on past deoxygenation (Nwosu, 2022). Similarly, in Lake Bourget (France) and Lake Geneva (Switzerland), XRF scanning has been used to infer past oxygenation changes through Fe, Mn, and S fluctuations; however, these studies did not incorporate biological data from sedimentary DNA analyses (Jenny et al., 2014; Giguet-Covex et al., 2010).

Our data reveal a marked intensification of lake stratification between 1963 and 2006, leading to extended meromictic conditions. Despite differences in methodology, this pattern aligns with previous research on climate-driven lake deoxygenation. Jenny et al. (2016) and Jansen et al. (2024) documented similar trends beginning in the mid-XXth century, confirming prolonged stratification and declining oxygen levels. Similarly, Huang et al. (2022) identified an increasing frequency of hypoxic events since the 1950s, reinforcing our interpretations. Additional support comes from Müller et al. (2012), Jane et al. (2021)Iwańska et al., 2022; and Zhang et al. (2023); (2025), all of whom reported intensified deoxygenation in overlapping periods.The agreement of our findings with these independent studies validates our results and highlight their broader significance in understanding climate-driven stratification and oxygen loss over time.

The timing of stratification intensification in Lake Montcortès aligns with the onset of the Anthropocene epoch, as defined by the Anthropocene Working Group (AWG), which places its boundary in the mid-20th century during the Great Acceleration—a period of rapid, human-driven change. Owing to absolute annual-resolution dating over the last century and the extensive research conducted to date, Lake Montcortès has been proposed as a candidate Global Boundary Stratotype Section and Point (GSSP) (Rull and Vegas-Vilarrúbia, 2023). Our findings support this proposal, revealing distinct geochemical and microbial signals of anthropogenic impact and microbial adaptation to prolonged oxygen limitation.

5. Conclusions

The reconstructed trends show a slight increase in average volume of anoxic bottom water and a pronounced decline in variability, from the preindustrial to the postindustrial period. Despite the semiquantitative nature of the method, the results are coherent and indicate a shift toward more stable and persistent anoxic conditions, likely driven by sustained climatic and anthropogenic forcing.

Reconstruction of microbial communities over the past five centuries reveals gradual yet structured shifts in dominant redox-sensitive bacterial taxa. These changes reflect intermittent mixing events and a long-term intensification of bottom-water anoxia, driven by both climatic variability and anthropogenic influence

While Lake Montcortès has remained meromictic for millennia, external pressures—including historical hemp retting and cultivation, erosion-driven organic input, and recent climate warming—have progressively reinforced stratification and deoxygenation in the monimolimnion. These transitions are mirrored in the microbial community by a functional reorganization favoring anaerobic metabolic pathways, including sulfate reduction and the occasional presence of methanogenesis-associated taxa.

Despite these shifts, we find evidence of ecological resilience and functional continuity. Certain bacterial groups persist across

environmental phases, suggesting legacy effects and adaptation under stable redox constraints. The integration of sedimentary ancient DNA (sedDNA) with high-resolution sediment archives offers new insights into how aquatic microbiomes reorganize under prolonged environmental stress—contributing to our understanding of microbial stability and feedback in a changing climate.

The long-term perspective offered by the Montcortès record reveals how sustained stratification and progressive deoxygenation can reshape microbial ecosystems towards anaerobic dominance. Given the ongoing expansion of anoxic water masses in lakes and coastal zones, such trajectories may not remain exceptional. Instead, they may become increasingly common as climate warming intensifies. Therefore, understanding microbial long-term dynamics under persistent anoxia is essential for anticipating future shifts in lacustrine ecosystem functioning.

By capturing microbial responses to oxygen variability since 1500 CE, our study bridges an important knowledge gap between short-term observations and long-term ecosystem transformations. These findings demonstrate how progressive deoxygenation and redox stratification can drive structural and functional microbial changes over centennial timescales, reinforcing concerns about the future expansion of anoxic zones in aquatic systems under continued climate forcing.

Lake Montcortès captures distinct biological and geochemical signals of mid-20th-century anthropogenic change, supporting its suitability as a stratigraphic marker for the proposed onset of the Anthropocene epoch.

CRediT authorship contribution statement

Teresa Vegas-Vilarrúbia: Writing – review & editing, Writing – original draft, Supervision, Resources, Project administration, Methodology, Investigation, Funding acquisition, Formal analysis, Conceptualization. **Oriol Sacristán-Soriano**: Writing – review & editing, Writing – original draft, Methodology, Investigation, Formal analysis. **Carles M. Borrego**: Writing – review & editing, Writing – original draft, Methodology, Investigation, Funding acquisition, Formal analysis, Conceptualization. **Pablo Corella**: Writing – review & editing, Methodology, Investigation, Formal analysis. **Paz Errea**: Writing – review & editing, Methodology, Investigation, Formal analysis. **Teresa Buchaca**: Writing – review & editing, Investigation. Valentí Rull: Writing – review & editing, Writing – original draft, Methodology, Investigation, Formal analysis.

Declaration of Competing Interest

The authors declare that they have no known competing financial interests or personal relationships that could have appeared to influence the work reported in this paper.

Acknowledgements

This research was supported by the Spanish Ministry of Economy and Competitiveness (MINECO/FEDER) through the projects MONT500 (Ref. CGL2012-33665), MEROMONT (Ref. CGL2017-85682-R) and GLOBALKARST (Ref. CGL2009-08145); Agència de Gestió d'Ajuts Universitaris i de Recerca (AGAUR) through the Consolidated Research Groups 2021 SGR 01282 ICRA-ENV and 2021 SGR 00315; and additional support from the CERCA Programme/Generalitat de Catalunya. Authors thank the Council of Baix Pallars for facilitating access to the lake; Josep Fillat and Marc Pedrals from Club Busseing Pallars for their direct involvement in the project and ongoing logistical support. We gratefully acknowledge Eric Puche, Mª Carmen Trapote, Eric Tornabella, Arnau Blasco and Joan Gomà for their invaluable assistance in the laboratory and during fieldwork.

Appendix A. Supporting information

Supplementary data associated with this article can be found in the online version at doi:10.1016/j.ancene.2025.100504.

Data availability

Data will be made available on request.

References

Aben, R.C.H., Barros, N., Van Donk, E., Frenken, T., Hilt, S., Kazanjian, G., Lamers, L.P. M., Peeters, E.T.H.M., Roelofs, J.G.M., Domis, L.N.D.S., Stephan, S., Velthuis, M., Van De Waal, D.B., Wik, M., Thornton, B.F., Wilkinson, J., DelSontro, T., Kosten, S., 2017. Cross continental increase in methane ebullition under climate change. Nat. Commun. 8 (1), 1682. https://doi.org/10.1038/s41467-017-01535-y.

Apprill, A., McNally, S., Parsons, R., Weber, L., 2015. Minor revision to V4 region SSU rRNA 806R gene primer greatly increases detection of SAR11 bacterioplankton. Aquat. Microb. Ecol. 75 (2), 129–137. https://doi.org/10.3354/ame01753.

Battarbee, R.W., 2000. Palaeolimnological approaches to climate change, with special regard to the biological record. Quat. Sci. Rev. 19 (1-5), 107–124. https://doi.org/10.1016/s0277-3791(99)00057-8.

Beaulieu, J.J., DelSontro, T., Downing, J.A., 2019. Eutrophication will increase methane emissions from lakes and impoundments during the 21st century. Nat. Commun. 10, 1375. https://doi.org/10.1038/s41467-019-09100-5.

Bennett, K.D., 1992. Psimpoll—a quick basic program that generates postcript page description of pollen diagrams. INQUA Newsl. 8, 11–12.

Bennett, K.D., 1996. Determination of the number of zones in a biostratigraphical sequence. N. Phytol. 132 (1), 155–170. https://doi.org/10.1111/j.1469-8137.1996.tb04521.x.

Bisanz, J. (2018). jbisanz/qiime2R: Import qiime2 artifacts to R. GitHub.

Bleuze, L., Chabbert, B., Lashermes, G., Recous, S., 2020. Hemp harvest time impacts on the dynamics of microbial colonization and hemp stems degradation during dew retting. Ind. Crops Prod. 145, 112122. https://doi.org/10.1016/j.indcrop.2020.112122.

Boere, A.C., Damsté, J.S.S., Rijpstra, W.I.C., Volkman, J.K., Coolen, M.J.L., 2011. Source-specific variability in post-depositional DNA preservation with potential implications for DNA based paleoecological records. Org. Geochem. 42 (10), 1216–1225. https://doi.org/10.1016/j.orggeochem.2011.08.005.

Bolyen, E., Rideout, J.R., Dillon, M.R., Bokulich, N.A., Abnet, C.C., Al-Ghalith, G.A., Alexander, H., Alm, E.J., Arumugam, M., Asnicar, F., Bai, Y., Bisanz, J.E., Bittinger, K., Brejnrod, A., Brislawn, C.J., Brown, C.T., Callahan, B.J., Caraballo-Rodríguez, A.M., Chase, J., Caporaso, J.G., 2019. Reproducible, interactive, scalable and extensible microbiome data science using QIIME 2. Nat. Biotechnol. 37 (8), 852–857. https://doi.org/10.1038/s41587-019-0209-9.

Bou Orm, E., Bergeret, A., Malhautier, L., 2024. Microbial communities and their role in enhancing hemp fiber quality through field retting. Applied Microbiology and Biotechnology 108 (1), 501.

Boyle, J.F., 2001. Inorganic geochemical methods in palaeolimnology. In: Last, W.M., Smol, J.P. (Eds.), Tracking Environmental Change Using Lake Sediments. Volume 2: Physical and Geochemical Methods. Kluwer Academic Publishers, Dordrecht, pp. 83–141.

Breitburg, D., Levin, L.A., Oschlies, A., Grégoire, M., Chavez, F.P., Conley, D.J., Garçon, V., Gilbert, D., Gutiérrez, D., Isensee, K., Jacinto, G.S., Limburg, K.E., Montes, I., Naqvi, S.W.A., Pitcher, G.C., Rabalais, N.N., Roman, M.R., Rose, K.A., Seibel, B.A., Zhang, J., 2018. Declining oxygen in the global ocean and coastal waters. Science 359 (6371), eaam7240. https://doi.org/10.1126/science.aam7240.

Brooks, S.J., Langdon, P.G., Heiri, O., 2001. The identification and use of palaearctic chironomidae larvae in palaeoecology. Quat. Res. 29, 213–231.

Bush, T., Diao, M., Allen, R.J., Sinnige, R., Muyzer, G., Huisman, J., 2017. Oxic-anoxic regime shifts mediated by feedbacks between biogeochemical processes and microbial community dynamics. Nat. Commun. 8 (1), 789. https://doi.org/10.1038/s41467-017-00912-x.

Caporaso, J.G., Lauber, C.L., Walters, W.A., Berg-Lyons, D., Lozupone, C.A., Turnbaugh, P.J., Fierer, N., Knight, R., 2011. Global patterns of 16S rRNA diversity at a depth of millions of sequences per sample. Proc. Natl. Acad. Sci. USA 108 Suppl 1 (Suppl 1), 4516–4522. https://doi.org/10.1073/pnas.1000080107.

Carini, P., Marsden, P.J., Leff, J.W., Morgan, E.E., Strickland, M.S., Fierer, N., 2016. Relic DNA is abundant in soil and obscures estimates of soil microbial diversity. Nat. Microbiol. 2 (3), 16242. https://doi.org/10.1038/nmicrobiol.2016.242.

Chen, N., Bianchi, T.S., McKee, B.A., Bland, J.M., 2001. Historical trends of hypoxia on the Louisiana shelf: Application of pigments as biomarkers. Org. Geochem. 32 (4), 543–561. https://doi.org/10.1016/s0146-6380(00)00194-7.

Chiang, E., Schmidt, M.L., Berry, M.A., Biddanda, B.A., Burtner, A., Johengen, T.H., Palladino, D., Denef, V.J., 2018. Verrucomicrobia are prevalent in north-temperate freshwater lakes and display class-level preferences between lake habitats. PLoS One 13 (3), e0195112. https://doi.org/10.1371/journal.pone.0195112.

Corella, J.P., Benito, G., Rodriguez-Lloveras, X., Brauer, A., Valero-Garcés, B.L., 2014. Annually-resolved lake record of extreme hydro-meteorological events since AD 1347 in NE Iberian Peninsula. Quat. Sci. Rev. 93, 77–90. https://doi.org/10.1016/j.quascirev.2014.03.020.

Corella, J.P., Benito, G., Wilhelm, B., Montoya, E., Rull, V., Vegas-Vilarrúbia, T., Valero-Garcés, B.L., 2019. A millennium-long perspective of flood-related seasonal sediment

yield in Mediterranean watersheds. Glob. Planet. Change 177, 127–140. https://doi.org/10.1016/j.gloplacha.2019.03.016.
Corella, J.P., Moreno, A., Morellón, M., Rull, V., Giralt, S., Rico, M.T., Pérez-Sanz, A., Valero-Garcés, B.L., 2011. Climate and human impact on a meromictic lake during the last 6,000 years (Montcortès Lake, Central Pyrenees, Spain). Journal of Paleolimnology 46, 351–367.
Davies, S.J., Lamb, H.F., Roberts, S.J., 2015. Micro-XRF core scanning in palaeolimnology: Recent developments. In: Croudace, I.W., Rothwell, R.G. (Eds.), Micro-XRF studies of sediment cores: Applications of a non-destructive tool for the environmental sciences. Springer, pp. 189–226.
Davison, W., 2003. Iron and manganese in lakes. Earth Science Reviews 57, 347–370.
De Vries, A., & Ripley, B.D. (2024). ggdendro: Create dendrograms and tree diagrams using 'ggplot2'. R package version 0.2.0. ⟨https://andrie.r-universe.dev/ggdendro⟩.
Djemiel, C., Maron, P.-A., Terrat, S., Dequiedt, S., Cottin, A., Ranjard, L., 2022. Inferring microbiota functions from taxonomic genes: a review. GigaScience 11, giab090. https://doi.org/10.1093/gigascience/giab090.
Dommain, R., Andama, M., McDonough, M.M., Prado, N.A., Goldhammer, T., Potts, R., Maldonado, J.E., Nkurunungi, J.B., Campana, M.G., 2020. The challenges of reconstructing tropical biodiversity with sedimentary ancient DNA: A 2200-year-long metagenomic record from Bwindi impenetrable forest, Uganda. Front. Ecol. Evol. 8, 218. https://doi.org/10.3389/fevo.2020.00218.
Dorado-Liñán, I., Büntgen, U., González-Rouco, F., Zorita, E., Montávez, J.P., Gómez-Navarro, J.J., Brunet, M., Heinrich, I., Helle, G., Gutiérrez, E., 2012. Estimating 750 years of temperature variations and uncertainties in the Pyrenees by tree-ring reconstructions and climate simulations. Climate 8 (3), 919–933. https://doi.org/10.5194/cp-8-919-2012.
Ficker, H., Luger, M., Pamminger-Lahnsteiner, B., Achleitner, D., Jagsch, A., 2017. From dimictic to monomictic: Empirical evidence of thermal regime transitions in three deep alpine lakes in Austria induced by climate change. Freshw. Biol. 62, 413–424. https://doi.org/10.1111/fwb.12874.
Fox, J., Wesiberg, S., Price, B., & Adler, D. (2021). Companion to applied regression [R package car version 3.0-12]. Sage.
Fu, J., Mueller, H., De Castro, J.V., Yu, C., Cavaco-Paulo, A., Guebitz, G.M., Nyanhongo, G.S., 2011. Changes in the bacterial community structure and diversity during bamboo retting. Biotechnol. J. 6 (10), 1262–1271. https://doi.org/10.1002/biot.201100105.
Giguet-Covex, C., Arnaud, F., Poulenard, J., et al., 2010. Sedimentological and geochemical records of past trophic state and hypolimnetic anoxia in large, hard-water Lake Bourget, French Alps. J. Paleolimnol. gy 43, 171–190. https://doi.org/10.1007/s10933-009-9324-9.
Glaubitz, S., Labrenz, M., Jost, G., Jürgens, K., 2010. Diversity of active chemolithoautotrophic prokaryotes in the sulfidic zone of a Black sea pelagic redoxcline as determined by rRNA-based stable isotope probing. FEMS Microbiol. Ecol. 74 (1), 32–41. https://doi.org/10.1111/j.1574-6941.2010.00944.x.
Gloor, G.B., Macklaim, J.M., Pawlowsky-Glahn, V., Egozcue, J.J., 2017. Microbiome datasets are compositional: and this is not optional. Front. Microbiol. 8, 2224. https://doi.org/10.3389/fmicb.2017.02224.
Grote, J., Jost, G., Labrenz, M., Herndl, G.J., Jürgens, K., 2008. Epsilonproteobacteria represent the major portion of chemoautotrophic bacteria in sulfidic waters of pelagic redoxclines of the Baltic and Black seas. Appl. Environ. Microbiol. 74 (24), 7546–7551. https://doi.org/10.1128/AEM.01186-08.
Hammer, Ø., Harper, D.A., 2001. Past: Paleontological statistics software package for educaton and data anlysis. Palaeontol. Electron. 4 (1), 1.
Hervé, M. (2021). "RVAideMemoire": Testing and plotting procedures for biostatistics (0.9-81). ⟨https://CRAN.R-project.org/package=RVAideMemoire⟩.
Hill, M.O., Gauch, H.G., 1980. Detrended correspondence analysis: an improved ordination technique. Vegetatio 42, 47–58.
Horne, A.J., Faisst, W.K., 2022. Hypolimnetic oxygenation 6: improvement in fisheries, hydropower, and drought management with costs of installation and operation in Camanche Reservoir, California, United States. Lake Reserv. Manag. 38 (3), 268–285. https://doi.org/10.1080/10402381.2022.2049404.
Huang, S., Zhang, K., Lin, Q., Liu, J., Shen, J., 2022. Abrupt ecological shifts of lakes during the anthropocene. Earth Sci. Rev. 227, 103981. https://doi.org/10.1016/j.earscirev.2022.103981.
Idescat. (2010). Territorial code 250390 — Baix Pallars: Statistical nomenclature of population entities of Catalonia (as of 01-01-2010). Statistical Institute of Catalonia. Accessed July 2025. https://www.idescat.cat/codis/?id=50&n=9&c=250390&t=5-9-2010.
Intergovernmental Panel on Climate Change (IPCC), 2021. Climate Change 2021: The Physical Science Basis. Contribution of Working Group I to the Sixth Assessment Report of the Intergovernmental Panel on Climate Change. Cambridge University Press, Cambridge.
Iwańska, O., Latoch, P., Suchora, M., Pidek, I.A., Huber, M., Bubak, I., Kopik, N., Kovalenko, M., Gąsiorowski, M., Armache, J.P., Starosta, A.L., 2022. Lake microbiome and trophy fluctuations of the ancient hemp rettery. Sci. Rep. 12 (1), 8846. https://doi.org/10.1038/s41598-022-12761-w.
Jane, S.F., Hansen, G.J.A., Kraemer, B.M., Leavitt, P.R., Mincer, J.L., North, R.L., Pilla, R. M., Stetler, J.T., Williamson, C.E., Woolway, R.I., Arvola, L., Chandra, S., DeGasperi, C.L., Diemer, L., Dunalska, J., Erina, O., Flaim, G., Grossart, H.P., Hambright, K.D., Rose, K.C., 2021. Widespread deoxygenation of temperate lakes. Nature 594 (7861), 66–70. https://doi.org/10.1038/s41586-021-03550-y.
Jane, S.F., Mincer, J.L., Lau, M.P., Lewis, A.S., Stetler, J.T., Rose, K.C., 2023. Longer duration of seasonal stratification contributes to widespread increases in lake hypoxia and anoxia. Glob. Change Biol. 29 (4), 1009–1023. https://doi.org/10.1111/gcb.16532.
Jansen, J., Simpson, G.L., Weyhenmeyer, G.A., Härkönen, L.H., Paterson, A.M., Del Giorgio, P.A., Prairie, Y.T., 2024. Climate-driven deoxygenation of northern lakes. Nat. Clim. Change 14 (8), 832–838. https://doi.org/10.1038/s41558.
Jenny, J.P., Arnaud, F., Alric, B., Dorioz, J.M., Sabatier, P., Meybeck, M., Perga, M.E., 2014. Inherited hypoxia: A new challenge for reoligotrophicated lakes under global warming. Glob. Biogeochem. Cycles 28, 1413–1423. https://doi.org/10.1002/2014GB004932.
Jenny, J.P., Arnaud, F., Dorioz, J.M., Giguet Covex, C., Frossard, V., Sabatier, P., Millet, L., Reyss, J.L., Tachikawa, K., Bard, E., Pignol, C., Soufi, F., Romeyer, O., Perga, M.E., 2013. A spatiotemporal investigation of varved sediments highlights the dynamics of hypolimnetic hypoxia in a large hard-water lake over the last 150 years. Limnol. Oceanogr. 58 (4), 1395–1408. https://doi.org/10.4319/lo.2013.58.4.1395.
Jenny, J.P., Francus, P., Normandeau, A., Lapointe, F., Perga, M.E., Ojala, A., Schimmelmann, A., Zolitschka, B., 2016. Global spread of hypoxia in freshwater ecosystems during the last three centuries is caused by rising local human pressure. Glob. Change Biol. 22, 1481–1489. https://doi.org/10.1111/gcb.13193.
Koopmans, M.P., Köster, J., Van Kaam-Peters, H.M.E., Kenig, F., Schouten, S., Hartgers, W.A., De Leeuw, J.W., Sinninghe Damsté, J.S., 1996. Diagenetic and catagenetic products of isorenieratene: Molecular indicators for photic zone anoxia. Geochim. Et. Cosmochim. Acta 60 (22), 4467–4496. https://doi.org/10.1016/s0016-7037(96)00238-4.
Ladwig, R., Hanson, P.C., Dugan, H.A., Carey, C.C., Zhang, Y., Shu, L., Duffy, C.J., Cobourn, K.M., 2021. Lake thermal structure drives interannual variability in summer anoxia dynamics in a eutrophic lake over 37 years. Hydrol. Earth Syst. Sci. 25 (2), 1009–1032. https://doi.org/10.5194/hess-25-1009-2021.
Lepš, J., Šmilauer, P. (2003). Multivariate Analysis of Ecological Data Using CANOCO. Cambridge University Press, Cambridge.
Lewis, A.S.L., Lau, M.P., Jane, S.F., Rose, K.C., Be'eri-Shlevin, Y., Burnet, S.H., Clayer, F., Feuchtmayr, H., Grossart, H.P., Howard, D.W., Mariash, H., Martin, J.D., North, R.L., Oleksy, I., Pilla, R.M., Smagula, A.P., Sommaruga, R., Steiner, S.E., Verburg, P., Carey, C.C., 2024. Anoxia begets anoxia: a positive feedback to the deoxygenation of temperate lakes. Glob. Change Biol. 30 (1), e17046. https://doi.org/10.1111/gcb.17046.
Lin, X., Wakeham, S.G., Putnam, I.F., Astor, Y.M., Scranton, M.I., Chistoserdov, A.Y., Taylor, G.T., 2006. Comparison of vertical distributions of prokaryotic assemblages in the anoxic Cariaco Basin and Black sea by use of fluorescence in situ hybridization. Appl. Environ. Microbiol. 72 (4), 2679–2690. https://doi.org/10.1128/AEM.72.4.2679-2690.2006.
Mallorquí, N., Arellano, J.B., Borrego, C.M., Garcia-Gil, L.J., 2005. Signature pigments of green sulfur bacteria in lower Pleistocene deposits from the Banyoles lacustrine area (Spain). J. Paleolimnol. 34 (2), 271–280. https://doi.org/10.1007/s10933-005-3731-3.
Matchado, M.S., Rühlemann, M., Reitmeier, S., Kacprowski, T., Frost, F., Haller, D., Baumbach, J., List, M., 2024. On the limits of 16S rRNA gene-based metagenome prediction and functional profiling. Microb. Genom. 10, 001203. https://doi.org/10.1099/mgen.0.001203.
McMurdie, P.J., Holmes, S., 2013. Phyloseq: An R Package for Reproducible Interactive Analysis and Graphics of Microbiome Census Data. PLoS ONE 8, e61217.https://doi.org/10.1371/journal.pone.0061217.
Monchamp, M.E., Spaak, P., Domaizon, I., Dubois, N., Bouffard, D., Pomati, F., 2019. Homogenization of lake cyanobacterial communities over a century of climate change and eutrophication. Nat. Ecol. Evol. 3 (2), 327–336. https://doi.org/10.1038/s41559-017-0407-0.
Monchamp, M.E., Walser, J.C., Pomati, F., Spaak, P., 2016. Sedimentary DNA reveals cyanobacterial community diversity over 200 years in two Perialpine lakes. Appl. Environ. Microbiol. 84 (21), e02046–17. https://doi.org/10.1128/AEM.02174-1672.
Montoya, E., Rull, V., Vegas-Vilarrúbia, T., Corella, J.P., Giralt, S., Valero-Garcés, B., (2022). Grazing activities in the southern central Pyrenees during the last millennium as deduced from the non-pollen palynomorphs (NPP) record of Lake Montcortès.
Müller, B., Bryant, L.D., Matzinger, A., Wüest, A., 2012. Hypolimnetic oxygen depletion in eutrophic lakes. Environmental Science & Technology 46, 996–1003.
Noguerola, I., Picazo, A., Llirós, M., Camacho, A., Borrego, C.M., 2015. Diversity of freshwater *Epsilonproteobacteria* and dark inorganic carbon fixation in the sulphidic redoxcline of a meromictic karstic lake. FEMS Microbiol. Ecol. 91 (7), fiv086. https://doi.org/10.1093/femsec/fiv086.
Nwosu, E.C. (2022). Sedimentary DNA-based reconstruction of cyanobacterial communities from Lake Tiefer See, NE Germany, for the last 11,000 years (Doctoral Thesis). University of Potsdam, Faculty of Science, Institute of Biochemistry and Biology, and GFZ German Research Centre for Geosciences, Helmholtz Centre Potsdam, Germany.
Ogata, M., Masuda, R., Harino, H., Sakata, M.K., Hatakeyama, M., Yokoyama, K., Yamashita, Y., Minamoto, T., 2021. Environmental DNA preserved in marine sediment for detecting jellyfish blooms after a tsunami. Sci. Rep. 11 (1), 16830. https://doi.org/10.1038/s41598-021-94286-2.
Ojala, A.E.K., Francus, P., Zolitschka, B., Besonen, M., Lamoureux, S.F., 2012. Characteristics of sedimentary varve chronologies–a review. Quat. Sci. Rev. 66, 177–185.
Oksanen, J., Blanchet, F.G., Friendly, M., Kindt, R., Legendre, P., McGlinn, D., Minchin, P.R., O'Hara, R.B., Simpson, G.L., Solymos, P., Henry, M., Stevens, H., Szoecs, E., & Wagner, H. (2020). Vegan: Community ecology package. R package version 2.2-0. ⟨http://CRAN.Rproject.org/package=vegan⟩.
Palarea-Albaladejo, J., Martín-Fernández, J.A., 2015. zCompositions — R package for multivariate imputation of left-censored data under a compositional approach.

Chemom. Intell. Lab. Syst. 143, 85–96. https://doi.org/10.1016/j.chemolab.2015.02.019.
Parada, A.E., Needham, D.M., Fuhrman, J.A., 2016. Every base matters: Assessing small subunit rRNA primers for marine microbiomes with mock communities, time series and global field samples. Environ. Microbiol. 18 (5), 1403–1414. https://doi.org/10.1111/1462-2920.13023.
Philippot, L., Griffiths, B.S., Langenheder, S., Lemanceau, P., Prosser, J.I., Rillig, M.C., Schloter, M., Wagg, C., 2021. The ecological resilience of microbial communities. Nature Reviews Microbiology 19, 405–415.
R Core Team (2021). R: A language and environment for statisticalcomputing. R Foundation for Statistical Computing, Vienna, Austria. URL https://www.R-project.org/.
Rhodes, J., Hetzenauer, H., Frassl, M.A., Rothhaupt, K.-O., Rinke, K., 2017. Long-term development of hypolimnetic oxygen depletion rates in the large Lake Constance. Ambio 46 (5), 554–565. https://doi.org/10.1007/s13280-017-0896-3.
Rose, K.C., Ferrer, E.M., Carpenter, S.R., et al., 2024. Aquatic deoxygenation as a planetary boundary and key regulator of Earth system stability. Nat. Ecol. Evol. https://doi.org/10.1038/s41559-024-02448-y.
Rull, V., Sacristán-Soriano, O., Sànchez-Melsió, A., Borrego, C.M., Vegas-Vilarrúbia, T., 2022. Bacterial phylogenetic markers in lake sediments provide direct evidence for historical hemp retting. Quat. Sci. Rev. 295, 107803. https://doi.org/10.1016/j.quascirev.2022.107803.
Rull, V., Sigro, J., Vegas-Vilarrúbia, T., 2024. Cannabis pollen sources and dispersal in the Iberian Pyrenees during the last century: Preliminary results and proposals for future studies. Rev. Palaeobot. Palynol. 331, 105208. https://doi.org/10.1016/j.revpalbo.2024.105208.
Rull, V., Vegas-Vilarrúbia, T., 2023. A recent Cannabis pollen increase on the Iberian Pyrenees. Sci. Total Environ. 886, 163947. https://doi.org/10.1016/j.scitotenv.2023.163947.
Rull, V., & Vegas-Vilarrúbia, T. (2024). Vegetation and landscape dynamics of the Iberian Pyrenees durig the last 3000 years. The Montcortès palynological record. Springer Nature.
Savichtcheva, O., Debroas, D., Perga, M.E., Arnaud, F., Villar, C., Lyautey, E., Kirkham, A., Chardon, C., Alric, B., Domaizon, I., 2015. Effects of nutrients and warming on *Planktothrix* dynamics and diversity: a palaeolimnological view based on sedimentary DNA and RNA. Freshw. Biol. 60, 31–49. https://doi.org/10.1111/fwb.12465.
Seidel, L., Ketzer, M., Broman, E., Shahabi-Ghahfarokhi, S., Rahmati-Abkenar, M., Turner, S., Ståhle, M., Bergström, K., Manoharan, L., Ali, A., Forsman, A., Hylander, S., Dopson, M., 2022. Weakened resilience of benthic microbial communities in the face of climate change. ISME Commun. 2 (1), 21. https://doi.org/10.1038/s43705-022-00104-9.
Tamburini, E., León, A.G., Perito, B., Mastromei, G., 2015. Characterization of bacterial pectinolytic strains involved in the water retting process. Environ. Microbiol. 5 (9), 730–736. https://doi.org/10.1046/j.1462-2920.2003.00462.x.
ter Braak, C.J.F., 1986. Canonical correspondence analysis: a new eigenvector technique for multivariate direct gradient analysis. Ecology 67, 1167–1179.
ter Braak, C.J.F., Prentice, I.C., 1988. A theory of gradient analysis. Adv. Ecol. Res. 18, 271–317.
Teunisse, G.M. (2022). Fantaxtic-nested bar plots for phyloseq data. ⟨https://rdrr.io/github/gmteunisse/Fantaxtic/man/plot_nested_bar.html⟩.
Trapote, M.C. (2019). Modern-analog studies and high-resolution paleoenvironmental reconstruction of the last 500 years using the varved sediments of the Mediterranean Lake Montcortès (Central Pyrenees) (PhD Thesis). Universitat de Barcelona, Spain.
Tu, Z., Zhang, Y., Shi, K., Gong, S., Zhao, Z., 2024. Landsat data reveal lake deoxygenation worldwide. Water Res. 267, 122525. https://doi.org/10.1016/j.watres.2024.122525.
Vegas-Vilarrúbia, T., Corella, J.P., Pérez-Zanón, N., Buchaca, T., Trapote, M.C., López, P., Sigró, J., Rull, V., 2018. Historical shifts in oxygenation regime as recorded in the laminated sediments of Lake Montcortès (Central Pyrenees) support hypoxia as a continental-scale phenomenon. Sci. Total Environ. 612, 1577–1592. https://doi.org/10.1016/j.scitotenv.2017.08.148.
Vegas-Vilarrúbia, T., Corella, J.P., Sigró, J., Rull, V., Dorado-Liñan, I., Valero-Garcés, B., Gutiérrez-Merino, E., 2022. Regional precipitation trends since 1500 CE reconstructed from calcite sublayers of a varved Mediterranean lake record (Central Pyrenees). Sci. Total Environ. 826, 153773. https://doi.org/10.1016/j.scitotenv.2022.153773.
Vegas-Vilarrúbia, T., Rull, V., Trapote, M.D.C., Cao, M., Rosell-Melé, A., Buchaca, T., Gomà, J., López, P., Sigró, J., Safont, E., Cañellas, N., Garcés-Pastor, S., Giralt, S., Corella, J.P., Pérez-Zanón, N., 2020. Modern analogue approach applied to high-resolution varved sediments—a synthesis for Lake Montcortès (Central Pyrenees). Quaternary 3 (1), 1. https://doi.org/10.3390/quat3010001.
Yu, T., Wu, W., Liang, W., Wang, Y., Hou, J., Chen, Y., Elvert, M., Hinrichs, K.U., Wang, F., 2023. Anaerobic degradation of organic carbon supports uncultured microbial populations in estuarine sediments. Microbiome 11 (1), 81. https://doi.org/10.1186/s40168-023-01531-z.
Zhang, Y., Fu, H., Chen, H., Liu, Z., 2023. Climate-driven intensification of hypolimnetic deoxygenation in Lake Fuxian, a monomictic lake in South-Western China, since the 1990s. Ecol. Indic. 154, 110567. https://doi.org/10.1016/j.ecolind.2023.110567.
Zhang, Y., Shi, K., Woolway, R.I., Wang, X., Zhang, Y., 2025. Climate warming and heatwaves accelerate global lake deoxygenation. Sci. Adv. 11 (12), 5369. https://doi.org/10.1126/sciadv.adt5369.
Zhang, M., Xiao, Q., Zhang, Z., Gao, Y., Zhao, J., Pu, Y., et al., 2019. Methane flux dynamics in a submerged aquatic vegetation zone in a subtropical lake. Science of the Total Environment 672, 400–409.